Am J Cancer Res 2024;14(5):2055-2071
www.ajcr.us /ISSN:2156-6976/ajcr0154281

*Original Article*

# *NOLC1* was identified as a tumor suppressor gene in thyroid cancer and correlated with prognosis by bioinformatics

Fengguang Zhai[1*], Yuxuan Li[2*], Xia Luo[2], Xiaofeng Jin[1,2], Meng Ye[1]

*[1]The First Hospital of Ningbo University, Ningbo 315010, Zhejiang, China; [2]Department of Biochemistry and Molecular Biology, Health Science Center, Ningbo University, Ningbo 315211, Zhejiang, China. [*]Equal contributors.*

Received November 6, 2023; Accepted April 15, 2024; Epub May 15, 2024; Published May 30, 2024

**Abstract:** Thyroid cancer (THCA) is the most common endocrine malignancy, mainly affecting women's unilateral glandular lobes. However, for relapsed and distant metastasis of THCA patients, the existing early diagnosis and treatment methods were still insufficient, and a new method was urgently needed to diagnose and treat them. Nucleolar and coiled-body phosphoprotein 1 (NOLC1) was one of the most phosphorylated proteins in the cell, which was located mainly in the nucleolus. In addition, more and more studies have confirmed that NOLC1 plays a crucial role in various pathological processes, such as the occurrence and progression of cancer and viral infection. A previous study showed that NOLC1, as a member of RNA-binding protein, was significantly correlated with the prognosis of THCA patients. However, further exploration of NOLC1 in THCA is limited. To further explore the role of NOLC1 in THCA, we conducted expression and survival prognosis analysis of NOLC1 using multiple databases. We also evaluated the correlation between NOLC1 gene expression and clinical characteristics of THCA patients. Furthermore, we analyzed the relationship between NOLC1 and other genes, followed by enrichment analysis to investigate its metabolic pathways and molecular metabolism processes. Additionally, we examined the association between immune cell infiltration in tumor microenvironment and NOLC1. Notably, through vitro experiments, we confirmed the tumor suppressive effect of NOLC1 on the proliferation and migration of human THCA cells, providing evidence for clinical diagnosis of THCA. Furthermore, we confirmed the tumor suppressive effect of NOLC1 in vivo xenograft assay. To sum up, our results suggest that NOLC1 is a tumor suppressor gene for THCA.

**Keywords:** NOLC1, THCA, immune infiltration, biomarker, bioinformatics

## Introduction

Thyroid cancer (THCA) was the most common endocrine malignancy, mainly affecting women's unilateral glandular lobes [1]. Because of histological differences, THCA was classified as differentiated thyroid cancer (DTC) and anaplastic thyroid cancer (ATC), the former accounts for approximately 90% of all THCA patients [2]. Most DTC patients were treated with surgery and radioactive iodine therapy, and the long-term survival rate was excellent [3]. However, tumor recurrence and metastasis impede clinical treatment, which in turn leads to a poor prognosis. In addition, the malignant degree of ATC was high, and the etiology was still unclear. Most of them were related to fast progression and poor prognosis, and there was currently no effective treatment method [2]. For relapsed and distant metastasis of DTC patients and ATC patients, the existing early diagnosis and treatment methods were still insufficient, and a new method was urgently needed to diagnose and treat them.

Nucleolar and coiled-body phosphoprotein 1 (NOLC1) was one of the most phosphorylated proteins in the cell, which was located mainly in the nucleolus [4]. NOLC1 regulated various cellular life activities, including ribosome biosynthesis, cell cycle, transcriptional coactivation, etc. [5]. In addition, more and more studies have confirmed that NOLC1 plays a crucial role in various pathological processes, such as the occurrence and progression of cancer and viral infection [5-9]. Although several studies have

https://doi.org/10.62347/IYVV7581

shown that NOLC1 functions as an oncogenic protein. For example, NOLC1, as a transcriptional coactivator, coordinates with p53 to transcriptional up-regulate the expression and activity of MDM2, thus promoting the occurrence and development of nasopharyngeal carcinoma [10]. However, NOLC1, as a multifunctional protein, could also function as a tumor suppressor. For example, the cellular senescence-inhibited gene (CSIG) can bind the 5'-UTR of NOLC1 and promote its mRNA degradation, thus inhibiting the proliferation of Hepatoma cells [11]. Therefore, the role of NOLC1 may be dependent on the cancer environment. Jing Zhen et al.'s study showed that NOLC1, as a member of RNA-binding protein, was significantly correlated with the prognosis of THCA patients. However, further exploration of NOLC1 in THCA is limited [12].

To further explore the role of NOLC1, we conducted expression and survival prognosis analysis of NOLC1 using multiple databases. We also evaluated the correlation between NOLC1 gene expression and clinical characteristics of THCA patients. Furthermore, we analyzed the relationship between NOLC1 and other genes, followed by enrichment analysis to investigate its metabolic pathways and molecular metabolism processes. Additionally, we examined the association between immune cell infiltration in tumor microenvironment and NOLC1. Finally, through in vitro and vivo experiments, we confirmed the tumor suppressive effect of NOLC1 on the human THCA cells, providing evidence for clinical diagnosis of THCA.

## Materials and methods

### *Data collection and procession*

From The Cancer Genome Atlas (TCGA) database (https://portal.gdc.cancer.gov) to download 512 thyroid carcinoma patients and 59 cases of normal thyroid tissue RNA-seq data. The FPKM format was then converted to transcripts per million (TPM) formats. Clinical information and RNA-seq data are retained. Further data processing was carried out through R 4.2.1.

Paired sample processing: RNA-seq data of normal and adjacent tissues of 59 patients with THCA were extracted. R package: ggplot2 (3.3.6), stats (4.2.1), and car (3.1.0) were used for further analysis, and a paired sample T-test was performed.

Unpaired sample processing: The data of 59 normal tissues and 512 THCA patient tissues were analyzed by R package: ggplot2 (3.3.6), stats (4.2.1), car (3.1.0), and Wilcoxon rank sum test was used.

UALCAN: The correlation between mRNA levels of NOLC1 and clinical features of patients with THCA was presented through the UALCAN database (https://ualcan.path.uab.edu/).

GEPIA2: The GEPIA2 database analyzes RNA information from the TCGA and GTEx databases (https://gepia2.cancer-pku.cn/). The first 100 genes associated with NOLC1 were collected through the GEPIA2 database, and the correlation between NOLC1 and the first four genes was analyzed. In addition, GEPIA2 was used to analyze the correlation between NOLC1 mRNA expression level and survival prognosis of prostate cancer patients.

STRING: The STRING database searches networks of known or likely interacting proteins. The human NOLC1 binding protein network was presented through the STRING URL. The active interaction source is "Text mining and experimentation". Set the minimum interaction score to High confidence (0.7000) and max number of interactors to show: 1st shell: Set the maximum interaction number to no more than 50 interactors. All others are "default" (https://cn.string-db.org/cgi/network?taskId=b9nrKajKnooA&sessionId=bd03WMEg0Ajg).

HPA: The Human Protein Atlas database (HPA) database was used for protein expression-related databases (https://www.proteinatlas.org/). Tissue by HPA database module and the pathological module NOLC1 protein in normal thyroid tissue samples and expression in thyroid carcinoma tissue samples (https://www.proteinatlas.org/ENSG00000166197-NOLC1/).

Timer 2.0: The "Timer-Gene" module was used to explore the relationship between NOLC1 expression and immune infiltration level in patients with THCA. Meanwhile, different algorithms were used to analyze the correlation between NOLC1 expression and immune infiltration in TCGA using the "Immune-gene" module.

*Cell culture*

Thyroid normal cell lines Nthy-ori-3-1 and human THCA cell lines FTC-133, BCPAP, and TPC-1 were derived from the American Type Culture Collection (ATCC). Nthy-ori-3-1 was cultured in Roswell Park Memorial Institute 1640 (RPMI-1640, Zhongqiaoxinzhou, China, Cat No: ZQ-200) including 10% Fetal Bovine Serum (FBS Premium, PAN-Seratech). FTC-133, BCPAP, and TPC-1 were cultured in Dulbecco's Modified Eagle Medium (DMEM, Zhongqiaoxinzhou, China, Cat No: ZQ-100) including 10% Fetal Bovine Serum (Standard Quality, China, Cat No: FBSST-01033). All cell lines were cultured at 37°C with 5% $CO_2$.

*Plasmid construction and transfections*

For over-expression and cell infection, pCMV-NOLC1-3*FLAG, pCMV-Vector, PMD2G, and PSPAX2 was purchased from the MiaoLing plasmid platform. For knockout, sh-NOLC1 and sh-Control was purchased from QingKe biotechnology company (Shanghai, China). sh-NOLC1 sequence: CCGGCAGTTAAAGCTCAGACTAAAGCTCGAGCTTTAGTCTGAGCTTTAACTGTTTTTT. All transfection assays were carried out using Lipo6000TM Transfection Reagent (Beyotime, China, Cat No: C0526) following the manufacturer's instructions.

*Cell infection*

To establish constitutive sh-NOLC1 and sh-Control THCA cells (TPC-1 and BCPAP), sh-RNA targeting NOLC1 (Gene ID: 9221) and sh-Control were acquired from QingKe biotechnology company (Shanghai, China). Day 1: 293T inoculation: The number of 293T cells was inoculated into a 10 cm dish two days in advance so that the cells reached a fusion rate of ~80% on the day of transfection. Day 2: Before transfection, the old cell culture medium was discarded, cleaned with 3-5 mL PBS, and serum-free DMEM was added, and then balanced in the incubator. Transfection reagents are prepared in the following proportions: Mix 1 (melting 25 μg sh-NOLC1 or sh-Control, 7.5 μg PMD2G, and 15 μg PSPAX2 in 1000 μL serum-free DMEM). Mix 2 (melting 100 μL Lipo6000TM Transfection Reagent in 1000 μL serum-free DMEM). Mix 1 and Mix 2, respectively, at room temperature for 5-10 min, then Mix 1 and Mix 2, at room temperature for 30 min, and add to 10 cm dish. Day 3: Fresh medium (containing 10% FBS) was changed within 6 h-24 h to observe the transfection efficiency and take photos. Day 5: Observed cell state and photographed. The supernatant medium was collected and filtered through a 0.45 μm filter membrane. The supernatant medium was added into the ultra-fast centrifuge tube and then centrifuged at 25000 rpm at 4°C for 1.5 h after trimming. Discard the supernatant, redissolve with the appropriate virus preservation solution, mix, and dissolve overnight. Day 6: The virus was collected and packaged for virus titer determination. The collected viral supernatants were used to infect the THCA cells (Mixing with complete medium in 1:1 ratio). To achieve constitutive shRNA effects, puromycin selection was conducted to obtain stable sh-NOLC1 and sh-Control TPC-1 cells. Compared with stable sh-Control THCA cells, the low expression of NOLC1 in established constitutive sh-NOLC1 THCA cells has been proven at the protein level and RNA level.

*Western blotting*

Protein samples were obtained by using RIPA (high) Lysis Buffer (Meilunbio, China, Cat No: MA0153) with proteasome inhibitors. The protein samples were then subjected to 10% SDS-PAGE and transferred to the nitrocellulose membranes (Cat No: 10600001; Cytiva, USA). At room temperature, NC membranes were blocked with 5% fat-free milk for one hour. Membranes were probed with NOLC1 Polyclonal Antibody (Proteintech, China, Cat No: 11815-1-AP) and Recombinant Anti-GAPDH antibody (Servicebio, China, Cat No: GB15004-100) at 4°C overnight. HRP-conjugated secondary anti-rabbit antibody (SAB, China, Cat No: #L3012) infiltrates the NC membrane for one hour. The target proteins were developed on film using NcmECL Ultra (New Cell & Molecular Biotech, China, Cat No: P10300). At least two independent experiments, WB was conducted 2-3 times, and representativeness were given.

*Real-time quantitative PCR (RT-qPCR)*

By using TRIzol Reagent, total RNA was obtained from Nthy-ori-3-1, FTC-133, BCPAP, and TPC-1 cells (cat#15596018; Thermo Fisher, USA). cDNA was reverse-transcribed using HiScript III All-in-one RT SuperMix Perfect for qPCR (cat#R333; Vazyme, China). The Taq Pro Universal SYBR qPCR Master Mix (cat#Q712;

Vazyme, China) was used to PCR amplification. All data were quantitatively normalized by GAPDH. The primer sequences used for RT-qPCR are listed: GAPDH forward, 5'-GGTGGTCTCCTCTGACTTCAACA-3', reverse, 5'-GTTGCTGTAGCCAAATTCGTTGT-3'; NOLC1 forward, 5'-AAGAAGCCACAGAAGGTAGCA-3', reverse, 5'-CACTGGAGTCAGAAGAAGAAC-3'; casein kinase 2α1 (CSNK2A1) forward, 5'-GAACGCTTTGTCCACAGTGA-3', reverse, 5'-TATCGCAGCAGTTTGTCCAG-3'. At least two independent experiments, RT-qPCR was conducted 2-3 times, and representativeness were given.

*Colony formation assay*

TPC-1 and BCABP cell lines were inoculated in 6-well plates containing 2,000 individual cells per well in triplicate. After 14 days, the cells were fixed in 100% methanol for 5 min at room temperature and then stained with Giemsa dye for 20 min (Solarbio, China, cat#G1063). The images of cell colonies were captured using a scanner (CanoScan LiDE 300, Canon) and analyzed by Image J software. Each count was performed in triplicates.

*Transwell migration assay*

Transwell (Cat No: 3422; Costar, USA) was used to detect cell migration. The cells were starved in serum-free medium with 4,000 cells per chamber. After 18 h, the migrated cells underside of the filter was washed with PBS. The migrated cells were then stained in a shaker for 20 minutes with crystal violet solution (G4070, Solarbio, China). 4 fields were randomly selected and photographed with a 100× magnifying glass, and analyzed with Image J software.

*Cell proliferation assay*

Cell proliferation rates were determined using a Cell Counting Kit 8 (CCK-8) (cat#K1018; APExBIO, America) according to the manufacturer's instructions. 2,000 cells per well were inoculated in 96-well plates. During the incubation period of 1-7 days, 10 μL of CCK-8 solution was added to each cell culture, and the resulting OD values were measured at 450 nm using a microplate absorbance meter (Bio-Rad, Hercules, CA, USA) after 2 h of incubation. Each assay was performed in triplicates.

*Statistical analysis*

Statistical analyses were performed using GraphPad Prism 9 software. Comparisons between groups were made using Student's t-test. Multiple comparisons were analyzed using one-way analysis of variance (ANOVA). * represents $P < 0.05$; ** represents $P < 0.01$; *** represents $P < 0.001$; **** represents $P < 0.0001$.

*In vivo xenograft assay*

Four- to six-week-old NOD-SCID mice (strain No. T001492) (weighing 15-25 g) were obtained from Jiangsu GemPharmatech Co., Ltd. (Nanjing, China) for in vivo xenograft experiments. Prepare 4 portions of sh-NOLC1 TPC1 cells and 8 portions of sh-Control TPC1 cells in advance ($3 \times 10^6$ cells per portion). Two days before the in vitro experiment, the 8 parts sh-Control TPC1 cells were transiently transfected for FLAG-NOLC1 and EV (empty vector) plasmid respectively (10 μg per $3 \times 10^6$ cells). The 4 parts sh-NOLC1 TPC1 cells were transiently transfected for EV plasmid (10 μg per $3 \times 10^6$ cells). After digestion and centrifugation, each group of cells was re-suspended with 400 ul PBS, and 400 ul matrix glue (cat#082704; Mogengel, Xiamen, China) was added, and evenly distributed after mixing. Cultured TPC-1 cells grouped into sh-Control+EV, sh-Control+Flag-NOLC1, or sh-NOLC1+EV were subcutaneously transplanted into the right flank of 12 mice via randomization to groups (200 ul cell suspension per mouse). The tumor volume was measured every four days and ending in 16 days, starting four days post-transplantation, and calculated using the following formula: tumor volume = (long × wide$^2$) × 1/2. At the end of the experiment, the tumors were imaged and weighed after the mice were euthanized. A total of four mice were used in each group, and no blinding methods were used. All animal procedures were performed according to protocols approved by the Animal Care Committee of Ningbo University.

## Results

*Differential expression analysis of NOLC1 in thyroid carcinoma*

A flow chart shows the analysis of this study (**Figure 1**). By analyzing the matched and unmatched samples in the TCGA database, we found that the expression of NOLC1 in THCA was lower than that in adjacent tissues (**Figure 2A**, **2B**). Then, we collected one normal thyroid cell line (Nthy-ori-3-1) and three THCA cell lines

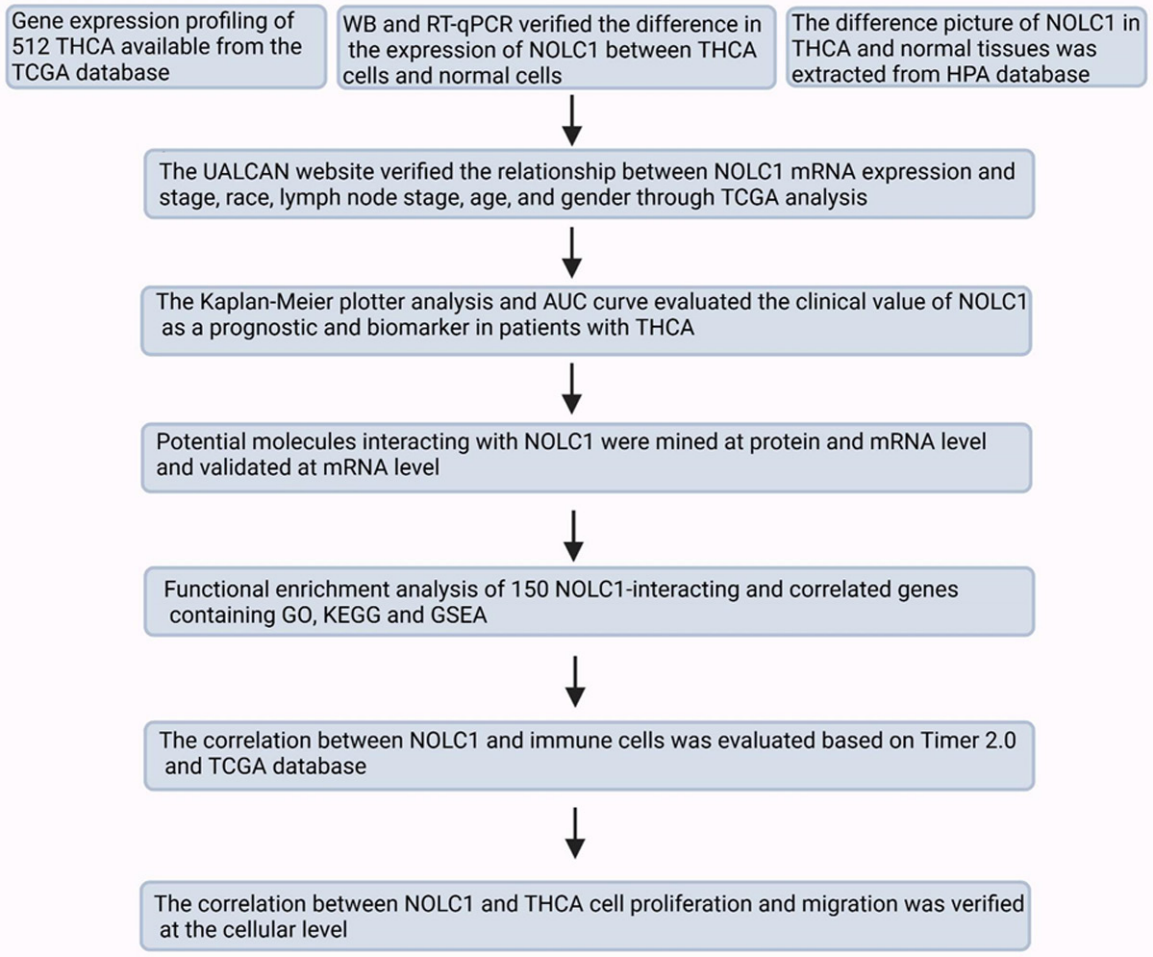


**Figure 1.** The flow chart of the analysis process.

(FTC-133, TPC-1, BCPAP) to detect the mRNA and protein levels of NOLC1, respectively (**Figure 2C**, **2D**). The results showed that NOLC1 protein and mRNA expression levels in normal thyroid cells were dramatically higher than those in THCA cells. Consistently, Human Protein Atlas database (HPA) database also indicated that NOLC1 protein was low expressed in THCA tissues (**Figure 2E**).

*Low expression of NOLC1 in THCA was related to clinical features and prognostic outcomes*

Clinical data of 510 patients with THCA were processed, including T stage, N stage, M stage, pathological stage, gender, age, race, histological type, Overall Survival (OS), Progression-free interval event (PFI), thyroid gland disorder history, neoplasm location, primary neoplasm focus type, extrathyroidal extension, residual tumor (**Table 1**). According to the chi-square test results, NOLC1 was closely correlated with T stage ($P < 0.001$), N stage ($P < 0.001$), pathological stage ($P < 0.001$), histological type ($P = 0.013$), thyroid gland disorder history ($P = 0.02$), primary neoplasm focus type ($P = 0.049$), and extrathyroidal extension ($P < 0.001$). While there was no significant correlation between NOLC1 expression and other clinicopathological features.

We used the UALCAN website to verify the relationship between NOLC1 mRNA expression and stage, race, lymph node stage, age, and gender through TCGA analysis (**Figure 3A-E**). The results showed that the lower the NOLC1 expression, the higher the stage, the more lymph node involvement, and the older the age. The expression of NOLC1 in male patients was lower than that in female patients (**Figure 3E**). Using the GEPIA2 database, according to the expression volume of NOLC1 (Custom High: 40;

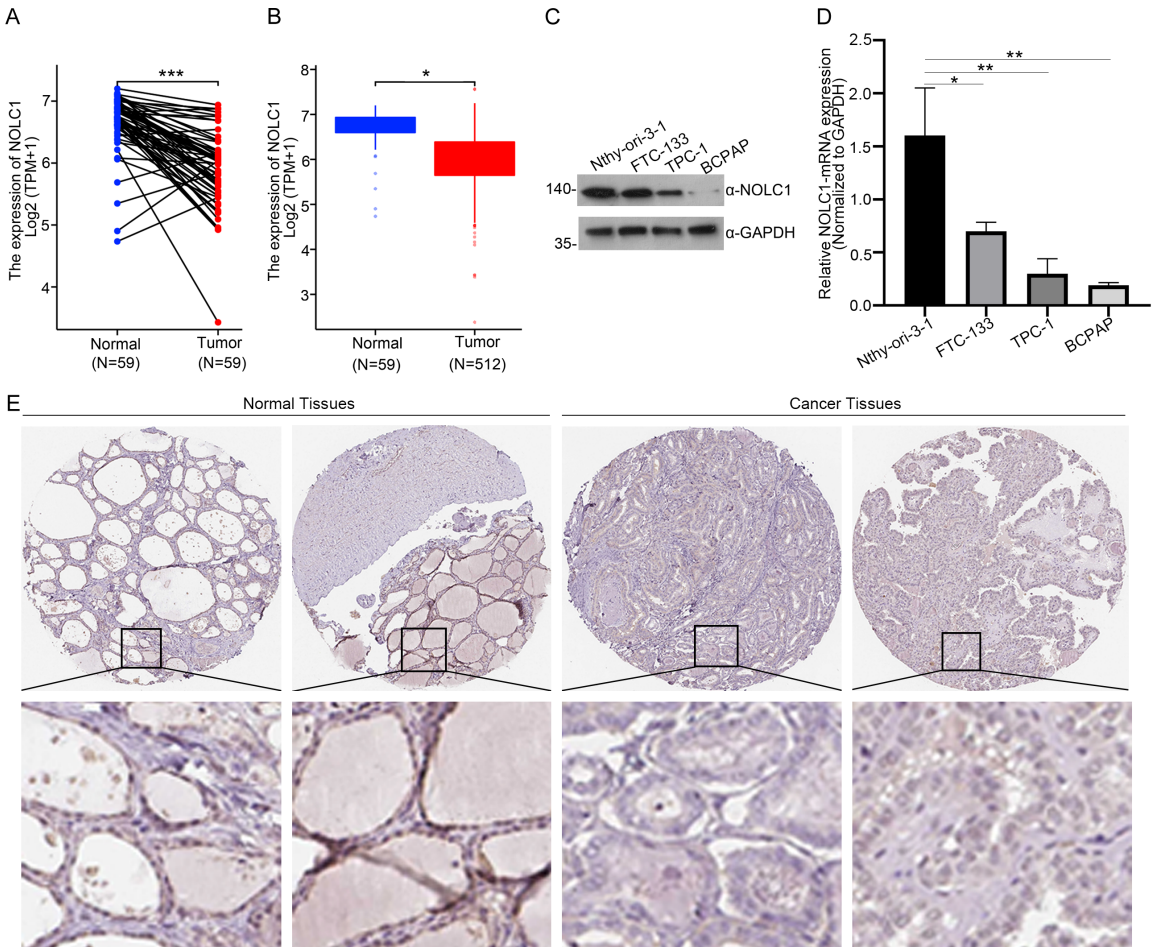


**Figure 2.** The expression level of NOLC1 in THCA. A. mRNA expression level of NOLC1 in 59 THCA tissues and adjacent paired tissues in TCGA. B. NOLC1 mRNA expression levels in cancerous and normal tissues in the TCGA THCA dataset. C. Western Blotting detected NOLC1 protein expression levels in normal and THCA cells. D. Detection of NOLC1 mRNA expression levels in normal and THCA cells by RT-qPCR. E. Comparison of NOLC1 between normal thyroid and THCA tissues based on the Human Protein Atlas database. *P*-value significant codes: *, $P < 0.05$; **, $P < 0.01$; ***, $P < 0.001$.

Custom Low: 60), The Kaplan-Meier plotter analysis showed that the Disease Free Survival (DFS) of THCA patients in the low NOLC1 group was worse than that in the high NOLC1 group ($P < 0.05$, **Figure 3F**). Receiver operating characteristic curve (ROC) analysis evaluated the diagnostic potential of NOLC1 for THCA and normal thyroid tissue (**Figure 3G**). The area under the ROC curve of NOLC1 in the TCGA database was 0.892 (95% CI: 0.838-0.947, $P < 0.0001$), suggesting that NOLC1 is a valuable diagnostic biomarker for THCA.

*Potential molecules interacting with NOLC1*

To explore the relationship between NOLC1 and other proteins in THCA, we used the STRING database to construct a protein-protein association (PPI) network (**Figure 4A**). In addition, to identify genes associated with *NOLC1* expression, we also obtained the top 100 genes from the GEPIA2 database. NOLC1 expression was positively correlated with the first four genes, 5-methylcytosine rRNA methyltransferase nsun-4 (NSUN4), DnaJ homolog subfamily C member 14 (DNAJC14), Ribosomal protein uL30-like (RPL7L1), and Regulation of nuclear pre-mRNA domain-containing protein 1B (RPRD1B) (**Figure 4B**). In addition, the expression of the above four genes in THCA was further detected, and the results showed that they were all low expressed in THCA (**Figure 4C**). The VENE diagram showed a common gene in the two groups of predicted gene sets, namely casein kinase 2α1 (CSNK2A1) (**Figure 4D**). CSNK2A1 was positively correlated with NOLC1

**Table 1.** Clinicopathological parameters of THCA patients with NOLC1 expression in TCGA

| Characteristic | Low expression of NOLC1 | High expression of NOLC1 | *P* |
|---|---|---|---|
| n | 255 | 255 | |
| T stage, n (%) | | | < 0.001 |
| T1 | 59 (11.6%) | 84 (16.5%) | |
| T2 | 74 (14.6) | 93 (18.3%) | |
| T3 | 102 (20.1) | 73 (14.4%) | |
| T4 | 19 (3.7) | 4 (0.8%) | |
| N stage, n (%) | | | < 0.001 |
| N0 | 96 (20.9) | 133 (28.9) | |
| N1 | 135 (29.3) | 96 (20.9) | |
| M stage, n (%) | | | 0.246 |
| M0 | 150 (50.8) | 136 (46.1) | |
| M1 | 7 (2.4) | 2 (0.7) | |
| Pathologic stage, n (%) | | | < 0.001 |
| Stage I | 129 (25.4%) | 157 (30.9%) | |
| Stage II | 20 (3.9%) | 32 (6.3%) | |
| Stage III | 63 (12.4) | 50 (9.8%) | |
| Stage IV | 42 (8.3%) | 15 (3%) | |
| Gender, n (%) | | | < 0.001 |
| Female | 167 (32.7%) | 204 (40%) | |
| Male | 88 (17.3%) | 51 (105%) | |
| Age, n (%) | | | 0.156 |
| ≤ 45 | 112 (22%) | 129 (25.3%) | |
| > 45 | 143 (28%) | 126 (24.7%) | |
| Race, n (%) | | | 0.934 |
| Asian | 25 (6%) | 26 (6.3%) | |
| Black or African American | 14 (3.4%) | 13 (3.1%) | |
| White | 174 (42%) | 162 (39.1%) | |
| Histological type, n (%) | | | 0.013 |
| Classical | 184 (36.1%) | 180 (35.3) | |
| Follicular | 41 (8%) | 60 (11.8%) | |
| Other | 4 (0.8%) | 5 (1%) | |
| Tall Cell | 26 (5.1%) | 10 (2%) | |
| OS event, n (%) | | | 0.799 |
| Alive | 248 (48.6) | 246 (48.2%) | |
| Dead | 7 (1.4%) | 9 (1.8%) | |
| PFI event, n (%) | | | 0.314 |
| Alive | 224 (43.9%) | 232 (45.5%) | |
| Dead | 7 (1.4%) | 9 (1.8%) | |
| Thyroid gland disorder history, n (%) | | | 0.02 |
| Lymphocytic Thyroiditis | 30 (6.6%) | 44 (9.7%) | |
| Nodular Hyperplasia | 25 (5.5%) | 43 (9.5%) | |
| Normal | 153 (33.8%) | 132 (29.2%) | |
| Other, specify | 15 (3.3%) | 10 (2.2%) | |
| Neoplasm location, n (%) | | | 0.065 |
| Bilateral | 34 (6.7%) | 54 (10.7%) | |
| Isthmus | 14 (2.8%) | 8 (1.6%) | |
| Left lobe | 89 (17.7%) | 88 (17.5) | |
| Right lobe | 116 (23%) | 101 (23%) | |

| | | | |
|---|---|---|---|
| Primary neoplasm focus type, n (%) | | | 0.049 |
| Multifocal | 105 (21%) | 128 (25.6%) | |
| Unifocal | 145 (29%) | 122 (24.4%) | |
| Extrathyroidal extension, n (%) | | | < 0.001 |
| No | 150 (30.5%) | 188 (38.2%) | |
| Yes | 94 (19.1%) | 60 (12.2%) | |
| Residual tumor, n (%) | | | 0.094 |
| R0 | 188 (42%) | 202 (45.1) | |
| R1 | 29 (6.5%) | 25 (5.6%) | |
| R2 | 4 (0.9%) | 0 (0%) | |

PFI: Progression-free interval event; OS: Overall Survival.

at the mRNA level and had lower expression in THCA (**Figure 4E**, **4F**). RT-qPCR results showed that NOLC1 and CSNK2A1 were positively correlated at the mRNA level (**Figure 4G**).

*Functional enrichment analysis of 150 NOLC1-interacting and correlated genes containing GO, KEGG and GSEA*

To explore the functional pathway of NOLC1 in THCA, a functional enrichment analysis of 150 NOLC1-related genes was presented (**Figure 5A-F**). Gene Ontology (GO) enrichment analysis, including biological processes (BP), cell composition (CC), and molecular function (MF), showed that these related genes were closely related to ribosome formation, rRNA metabolism, ribonucleoprotein generation, pre-ribosome and snoRNA binding (**Figure 5A**). In addition, the Kyoto Encyclopedia of Genes and Genomes (KEGG) pathway analysis showed that the pathways for significant enrichment of NOLC1-related genes included ribosome bioformation and RNA polymerase (**Figure 5B**). To further identify the biological function of NOLC1 in THCA, we performed GSEA identification of GO and KEGG pathways associated with NOLC1 on 150 gene sets related to NOLC expression. GO item GSEA showed a positive correlation with cardiac muscle tissue morphogenesis (**Figure 5C**). It negatively correlated with MHC class II protein complex (**Figure 5D**). GSEA in the KEGG pathway showed a positive correlation between Hedgehog signaling pathways, etc. (**Figure 5E**), and a negative correlation with allograft rejection, asthma, and intestinal immune network for IGA production, etc. (**Figure 5F**). Together, NOLC1 may be closely related to ribosome generation, antigen processing and presentation, and cell morphology in THCA.

*NOLC1 expression was associated with levels of immune cell infiltration in THCA*

The tumor microenvironment had been proven to be a vital factor in the occurrence and progression of cancers [13]. To further test the correlation between NOLC1 expression in THCA and immune cell infiltration, we sorted to analyze the data from the Timer 2.0 database. The results suggested that NOLC1 expression was positively correlated with CD8 T cells, CD4 T cells, macrophages, neutrophils, and dendritic cells (**Figure 6A**). Further, we investigated the correlation between the immune microenvironment and NOLC1 expression. According to the level of NOLC1 expression in THCA, 571 patients in the THCA dataset were divided into a high-expression group and a low-expression group. Then, the difference in expression levels of 24 immune cell subtypes in the high-low expression group was evaluated. The results showed that activated dendritic cells (ADCs), T cells, regulatory T cells (Tregs), and other immune cells were decreased in the group with low NOLC1 expression (**Figure 6B**). Meanwhile, we found that 6 among the above 24 kinds of immune cells, indicated a positive association with NOLC1 expression (**Figure 6C**).

*High expression of NOLC1 inhibits the occurrence and progression of THCA*

We first validated the protein levels and mRNA levels of FLAG-NOLC1 and sh-NOLC in TPC-1 and BCPAP cell lines, and selected sh-NOLC1#1 (hereinafter referred to as sh-NOLC1) with better effect (Supplementary Figure 1). By Western blotting (WB) and RT-qPCR, we confirmed the expression effect of FLAG-NOLC1, sh-NOLC1, and their corresponding control group in THCA. The results showed that both NOLC1 protein

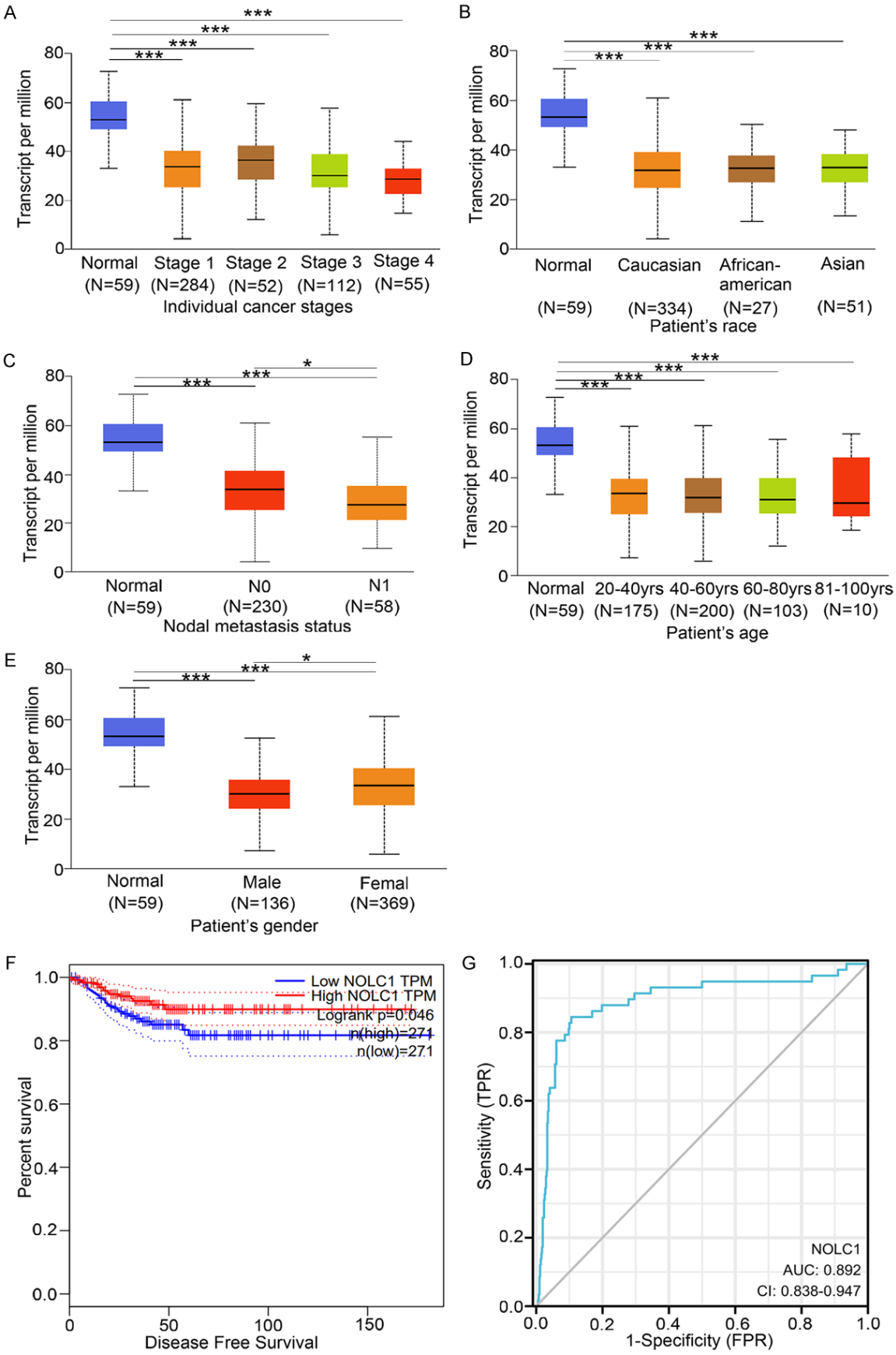
A
Transcript per million
Normal (N=59)
Stage 1 (N=284)
Stage 2 (N=52)
Stage 3 (N=112)
Stage 4 (N=55)
Individual cancer stages
B
Transcript per million
Normal (N=59)
Caucasian (N=334)
African-american (N=27)
Asian (N=51)
Patient's race
C
Transcript per million
Normal (N=59)
N0 (N=230)
N1 (N=58)
Nodal metastasis status
D
Transcript per million
Normal (N=59)
20-40yrs (N=175)
40-60yrs (N=200)
60-80yrs (N=103)
81-100yrs (N=10)
Patient's age
E
Transcript per million
Normal (N=59)
Male (N=136)
Femal (N=369)
Patient's gender
F
Low NOLC1 TPM
High NOLC1 TPM
Logrank p=0.046
n(high)=271
n(low)=271
Percent survival
Disease Free Survival
G
Sensitivity (TPR)
1-Specificity (FPR)
NOLC1
AUC: 0.892
CI: 0.838-0.947

**Figure 3.** Correlation between NOLC1 expression level and clinical features of THCA patients. A. Clinical stage. B. Race. C. Lymph node stage. D. Age. E. Gender. F. The Kaplan-Meier plotter analysis of NOLC1. G. The ROC curve shows the predictive value of NOLC1 to identify THCA tissue based on the TCGA database.

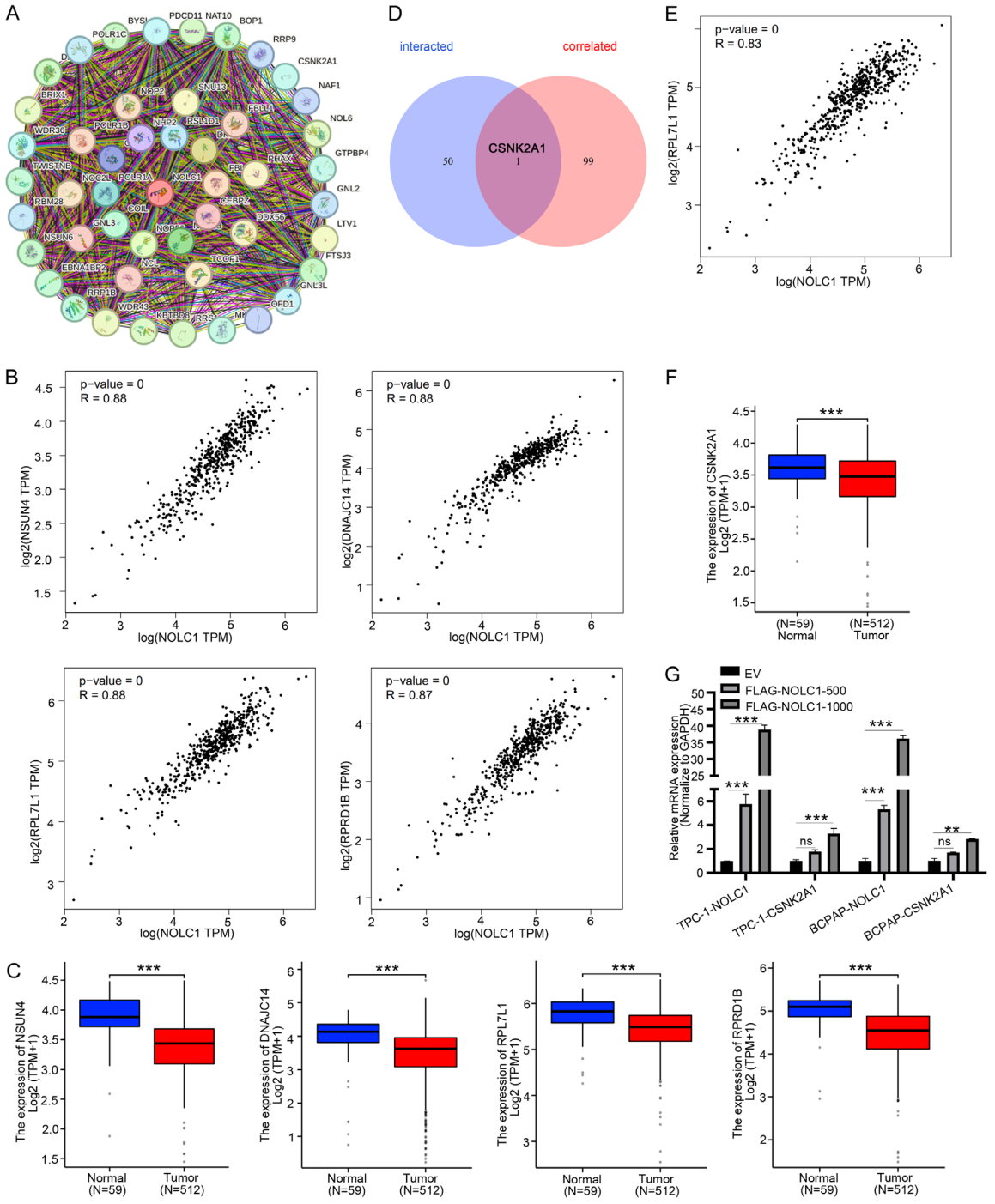


**Figure 4.** Potential molecules interacting with NOLC1. A. PPI network of NOLC1-binding proteins in STRING database. B. Correlation between NOLC1 and the top 4 NOLC1-related genes (including SUN4, DNAJC14, RPL7L1, RPRD1B) obtained from the top 100 NOLC1-related genes in the TCGA program in the GEPIA2 database. C. mRNA expression levels of the first 4 NOLC1-associated genes in cancer and normal tissues in the TCGA THCA dataset. D. Intersection analysis of NOLC1-interacting and correlated genes. E. Correlation between NOLC1 and CSNK2A1 at mRNA level. F. mRNA expression levels of CSNK2A1 in cancer and normal tissues in the TCGA THCA dataset. G. Detection of CSNK2A1 mRNA expression levels in normal and THCA cells by RT-qPCR. *P*-value significant codes: *, $P < 0.05$; **, $P < 0.01$; ***, $P < 0.001$.

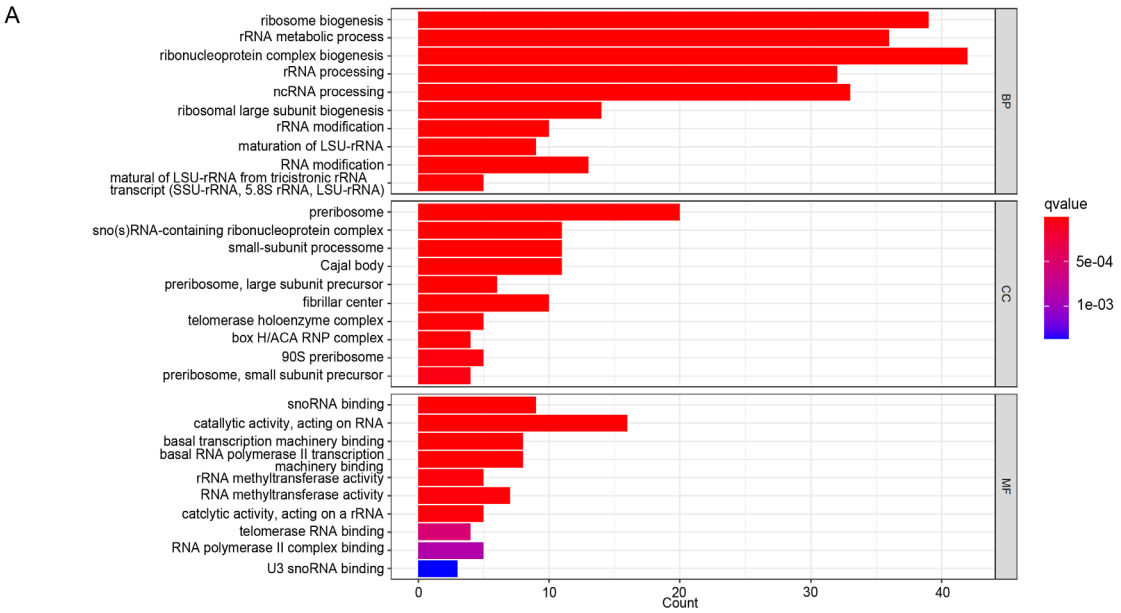
A
ribosome biogenesis
rRNA metabolic process
ribonucleoprotein complex biogenesis
rRNA processing
ncRNA processing
ribosomal large subunit biogenesis
rRNA modification
maturation of LSU-rRNA
RNA modification
matural of LSU-rRNA from tricistronic rRNA transcript (SSU-rRNA, 5.8S rRNA, LSU-rRNA)
preribosome
sno(s)RNA-containing ribonucleoprotein complex
small-subunit processome
Cajal body
preribosome, large subunit precursor
fibrillar center
telomerase holoenzyme complex
box H/ACA RNP complex
90S preribosome
preribosome, small subunit precursor
snoRNA binding
catallytic activity, acting on RNA
basal transcription machinery binding
basal RNA polymerase II transcription machinery binding
rRNA methyltransferase activity
RNA methyltransferase activity
catclytic activity, acting on a rRNA
telomerase RNA binding
RNA polymerase II complex binding
U3 snoRNA binding
BP
CC
MF
0
10
20
30
40
Count
qvalue
5e-04
1e-03

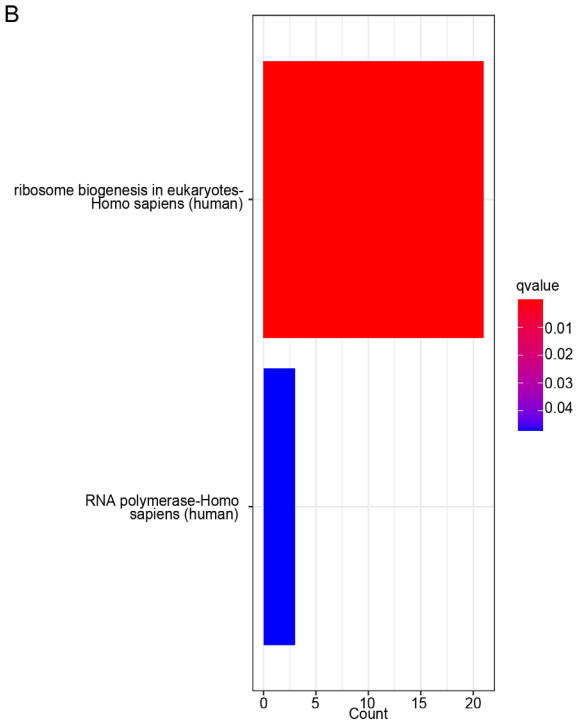
B
ribosome biogenesis in eukaryotes-Homo sapiens (human)
RNA polymerase-Homo sapiens (human)
0
5
10
15
20
Count
qvalue
0.01
0.02
0.03
0.04

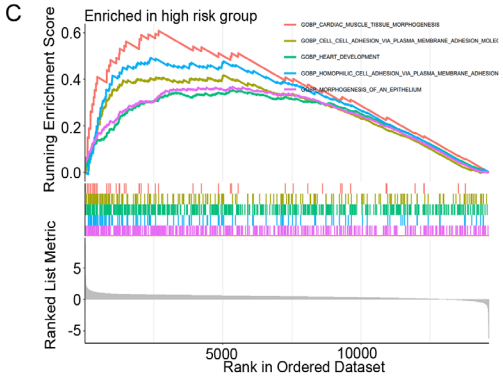
C
Enriched in high risk group
Running Enrichment Score
0.6
0.4
0.2
0.0
Ranked List Metric
5
0
-5
5000
10000
Rank in Ordered Dataset

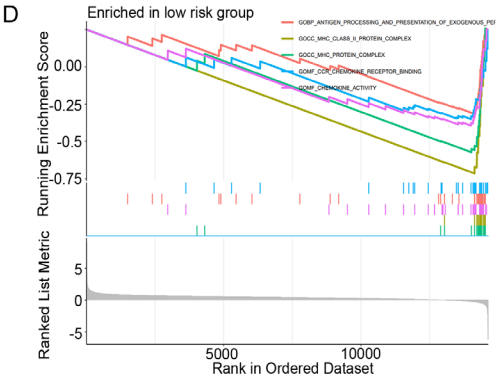
D
Enriched in low risk group
Running Enrichment Score
0.00
-0.25
-0.5
-0.75
Ranked List Metric
5
0
-5
5000
10000
Rank in Ordered Dataset

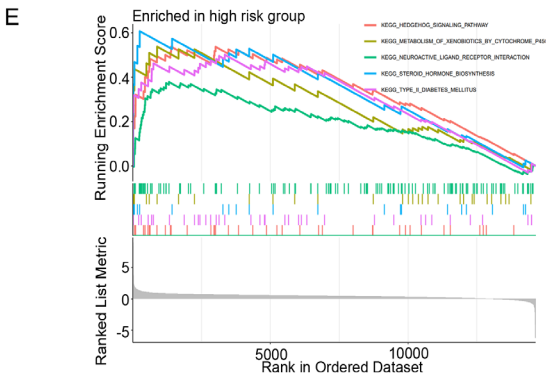
E
Enriched in high risk group
Running Enrichment Score
0.6
0.4
0.2
0.0
Ranked List Metric
5
0
-5
5000
10000
Rank in Ordered Dataset

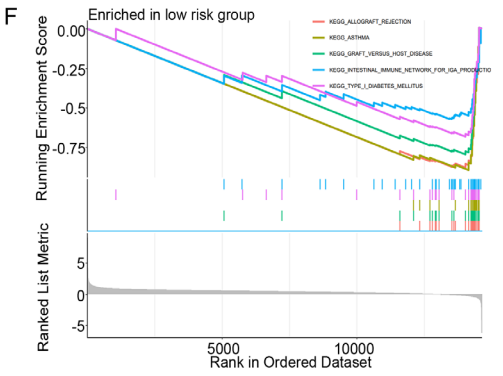
F
Enriched in low risk group
Running Enrichment Score
0.00
-0.25
-0.5
-0.75
Ranked List Metric
5
0
-5
5000
10000
Rank in Ordered Dataset

**Figure 5.** Functional enrichment analysis of 150 NOLC1-interacting and correlated genes contain Gene Ontology (GO), Kyoto Encyclopedia of Genes and Genomes (KEGG) pathway analysis, and Gene Set Enrichment Analysis (GSEA). A. GO enrichment analysis. B. KEGG pathway analysis. C-F. GSEA.

levels and mRNA levels could be increased or knockdown in both TPC-1 and BCPAP THCA cell lines (**Figure 7A-C**). To explore the effect of NOLC1 on the proliferation ability of THCA cells, we performed a CCK8 cell proliferation experiment and a colony formation experiment. Knockdown of *NOLC1* could promote the proliferation of THCA cells, while overexpression of NOLC1 significantly inhibited the proliferation ability of THCA cells (**Figure 7D-H**). To explore the effect of NOLC1 on the migration ability of THCA cells, the transwell migration experiment confirmed that knockdown of NOLC1 could promote the migration ability of THCA cells, while overexpression of NOLC1 significantly suppressed the migration ability of THCA cells (**Figure 7I-K**). To further verify the tumor inhibitory effect of *NOLC1* on THCA cells, we conducted tumor formation experiments in nude mice which showed that high expression of *NOLC1* could inhibit tumor growth (**Figure 7L-N**).

## Discussion

In recent years, the incidence and mortality of THCA, which occupies the first place of endocrine diseases, have increased year by year [14]. The main treatment of THCA is surgery, followed by endocrine therapy and radionuclide therapy [15]. For some patients with refractory THCA, there is still lack of effective treatment. At present, precise diagnosis and combination treatment are the key to improving survival. Therefore, there is an urgent need for biomarkers capable of early diagnosis and prediction of THCA. Previously, the continuous progress of basic research has made breakthroughs in individualized treatment. Doolittle et al. showed that CDK7 regulated the occurrence and development of THCA by regulating the NOTCH1-myc signaling axis, while CDK7 inhibitors can prevent the progression of THCA [16]. This discovery revealed an important signaling axis within THCA cells. Our findings suggest that NOLC1 is low-expressed in THCA and can serve as a biomarker for cancer development. However, the specific molecular mechanisms and functional characteristics of NOLC1 remain unclear. NOLC1 enables TRF2 to reside in the nucleolus, thereby enhancing the telomere binding activity of 53BP1, ultimately leading to telomere DNA damage response, cell cycle arrest and apoptosis. NOLC1 can induce telomere DNA damage response, cell cycle arrest and apoptosis by increasing TRF2 resident in the nucleolus which can enhance the telomere binding activity of 53BP1 [17, 18]. NOLC1 can be ubiquitinated by KBTBD8 to support the neural crest specification [19]. The function of NOLC1 is different in different tumor backgrounds. It has been reported that NOLC1, as an oncogene, can promote a variety of cancers including esophageal cancer, nasopharyngeal cancer and prostate cancer [5]. In addition, NOLC1 is involved in the resistance of hepatocellular carcinoma and renal clear cell carcinoma as a tumor suppressor gene [5].

Phosphorylation and ubiquitination are known to be important post-translational modification processes that regulate protein levels. Phosphorylation of serine at site 574 of NOLC1 protein leads to dysfunction of CK2α, which leads to the development of tumors. It has been found that the accumulation of downstream oncoproteins caused by the loss-of function mutation of E3 ligases or the continuous degradation of tumor suppressor proteins by some E3 ligase are essential factors leading to the development of cancer [20, 21]. For example, PCa-associated SPOP mutations lead to the accumulation of oncoproteins androgen (AR), c-MYC, ETS-related genes, and Egl family hypoxia-inducing factors, which contribute to the development and progression of prostate cancer [22]. Hypoxia induces SPOP accumulation to continuously degrade tumor suppressor proteins such as PTEN, ERK phosphatase, pro-apoptotic factor Daxx, and Gli2 transcription factor of the Hippo pathway [23]. Therefore, it is reasonable to consider that the low expression of NOLC1 in THCA is due to the dysregulation of its corresponding ubiquitination process. In addition, it has been reported that NOLC1 can be regulated by transcription factors such as NF-κB and CREB [24]. Our previous article summarized upstream molecules that may regulate NOLC1 transcription [5]. The upstream transcription factors that maintain the normal expression level of NOLC1 may also be regulat-

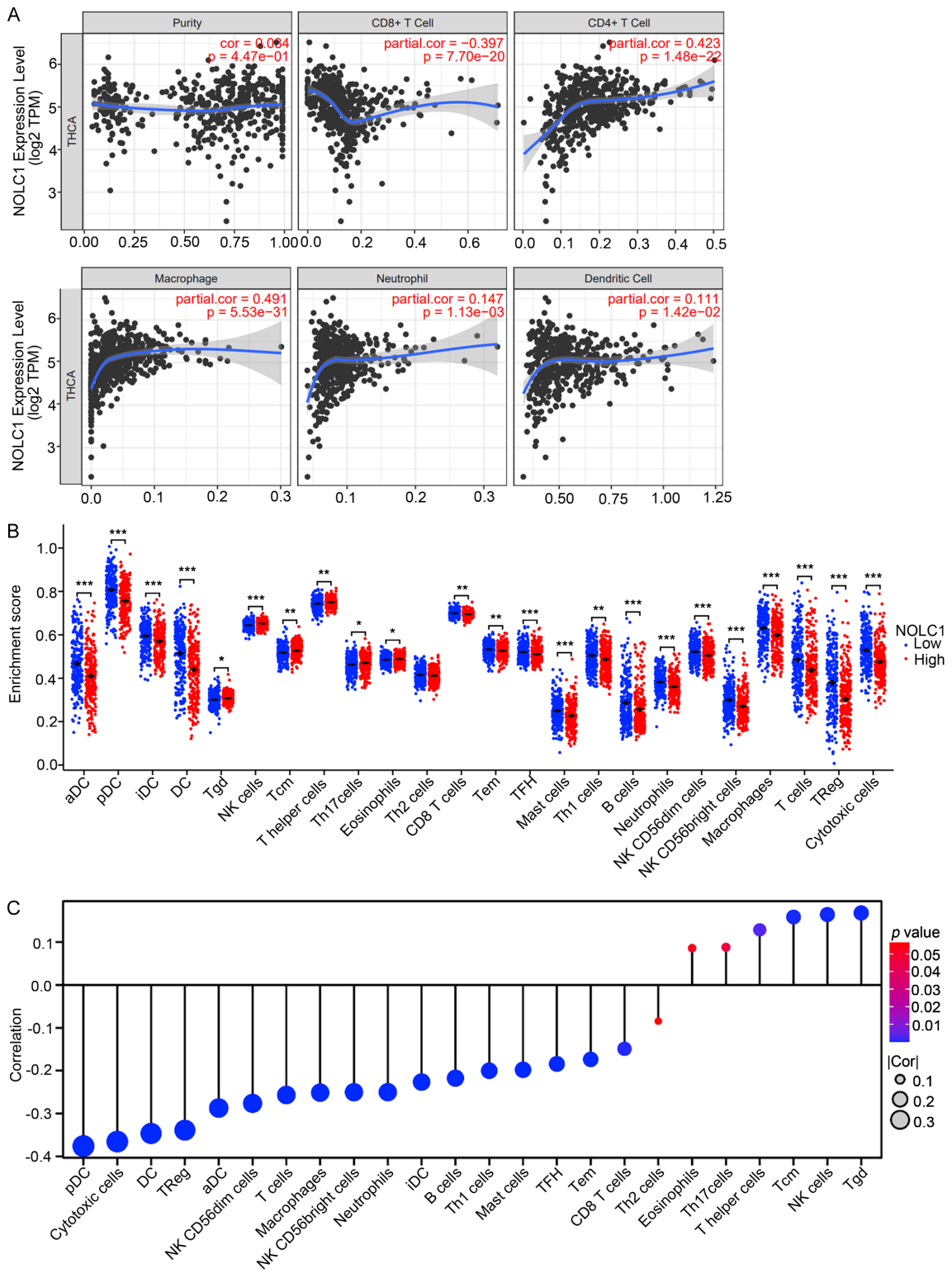


**Figure 6.** NOLC1 expression was associated with immune cell infiltration in THCA. A. Relationship between NOLC1 expression and immune infiltration level in the Timer 2.0 database. B. Twenty-four immune cells and their subtypes at different levels in the high and low NOLC1 expression groups in THCA tissue samples. C. The Spearman method was used to analyze the correlation between the infiltration level of 24 kinds of immune cells and NOLC1 expression in THCA tissues. pDC, plasmacytoid DC; DC, dendritic cell; TReg, regulatory T cell; aDC, activated DC; iDC, immature DC; Th, T helper cells; Th1, type 1 Th cell; TFH, T follicular helper; Tem, T effector memory; Th2, type 2 Th cells; Th17, type 17 Th cell; Tcm, T central memory; NK, natural killer; Tgd, T gamma delta.

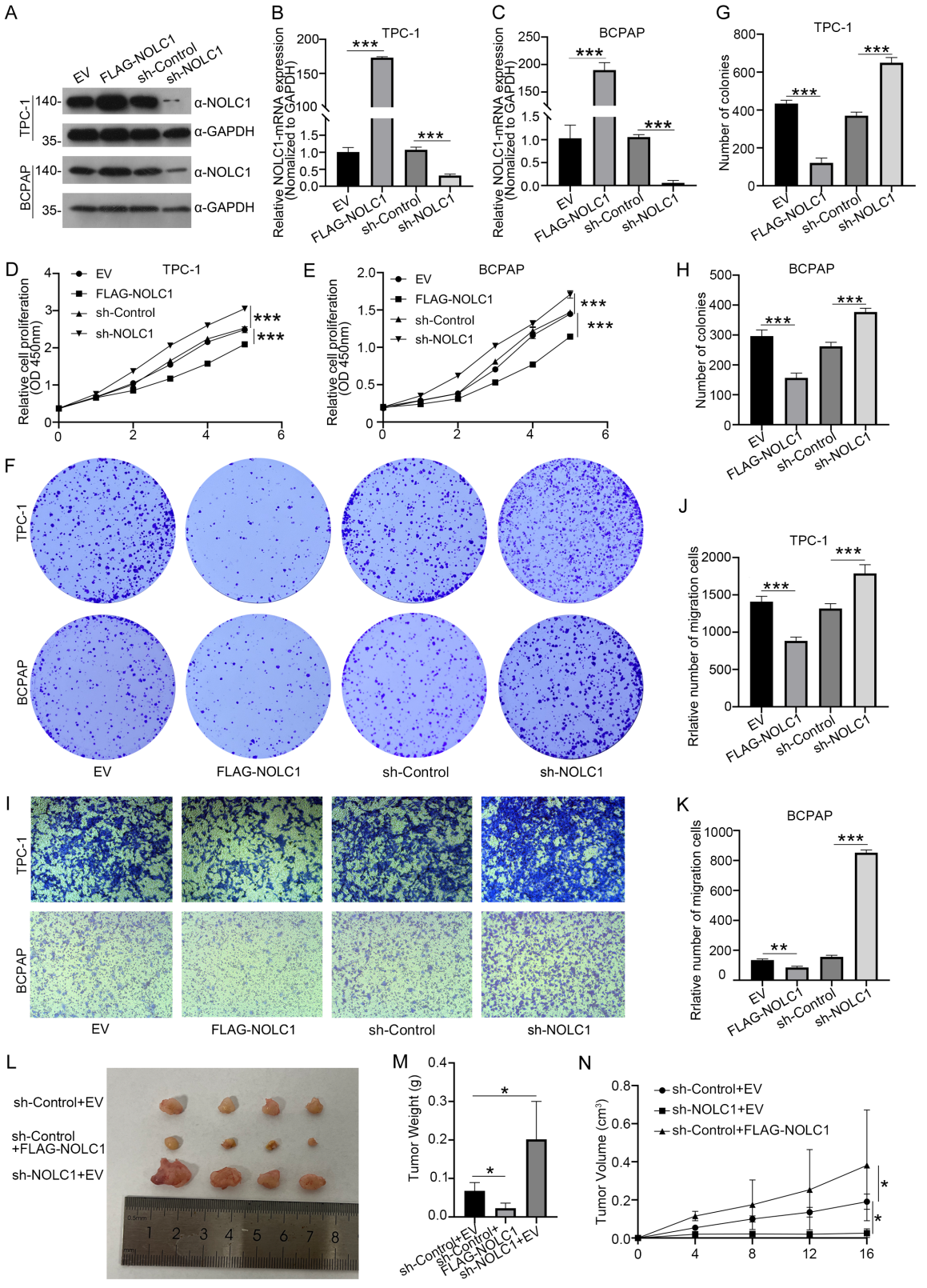


**Figure 7.** High expression of NOLC1 inhibited the proliferation and migration of THCA cells. A. Western Blotting evaluated the protein expression levels of NOLC1 in different THCA cell lines. B, C. RT-qPCR evaluated the mRNA expression level of NOLC1 in different THCA cell lines. D-H. The proliferation of THCA cells was detected by CCK-8 assay and colony formation assay. I-K. THCA cell migration was detected by transwell assay. L-N. Xenograft tumor model investigating the role of THCA cell (TPC-1) grouped into sh-Control+EV, sh-Control+Flag-NOLC1, or sh-NOLC1+EV. The data are presented as the means ± SDs for each group of mice (n = 4). *P*-value significant codes: *, $P < 0.05$; **, $P < 0.01$; ***, $P < 0.001$.

ed by ubiquitination process, thus indirectly reducing the expression of NOLC1.

Additionally, the tumor immune microenvironment is an essential part in the process of tumor occurrence and development and plays a dual role in tumor progression and host defense [25]. Our study showed that in the THCA tumor microenvironment with low NOLC1 expression, the abundance of various immune cells, including B cells, was higher, while the number of Th17 cells was lower. B cells are usually associated with tumorigenesis, and a mouse model confirms that aggregation of B-cell antibodies facilitates the development and spread of cancer [26]. In contrast, Th17 cells can recruit cytotoxic T cells and produce effector cytokines, including interferon-gamma, to induce anti-tumor immune responses [27, 28]. Therefore, we believe that the low expression of NOLC1 in THCA may affect the prognosis of THCA patients by altering the tumor microenvironment.

Although surgery is the primary treatment for patients with THCA, patients with refractory THCA or metastatic THCA require a more precise and individualized approach. In 2011, vandetanib was approved as the first THCA targeted drug. In 2020, anlotinib was approved as the 11th THCA targeted drug, which means that THCA targeted therapy is more accurate. The study by Subbinah et al. showed that the combination of dabrafenib and trametinib can significantly improve the long-term survival rate of patients with refractory THCA, providing a meaningful treatment option [29]. In addition, studies have shown that surufatinib combined with Toripalimab is also feasible as a neoadjuvant treatment for locally advanced THCA [30]. Despite the increasing availability of targeted therapy options, drug resistance can occur with long-term use. In previous studies, we found that NOLC1 overexpression increased the sensitivity of multidrug-resistant (MDR) cells to a variety of drug responses, such as 5-fluorouracil, paclitaxel, mitamycin, cisplatin, and gemcitabine hydrochloride. This suggests that NOLC1 is a potential target for increasing the sensitivity of multidrug-resistant cells.

However, there are some limitations in this experiment. First, although we collected representative images of THCA and NOLC1 protein expression levels in normal thyroid tissue from the HPA database, the number of cases in this database is still small at present. Second, most of the data came from public databases. Although we have demonstrated through some experiments that down-regulating the expression level of NOLC1 can promote the proliferation, migration and tumor formation of THCA cells, while increasing the expression level of NOLC1 can inhibit these processes, the downstream pathway of NOLC1 is still unclear. Finally, our experiments are limited to the phenotypic level. Studies are still needed to confirm the underlying mechanism of the anticancer effect of NOLC1 in THCA.

## Conclusion

In conclusion, our experiments confirmed that NOLC1 expression was reduced in THCA and could be used as a specific biomarker to distinguish THCA tissues from normal THCA tissues. Low expression of NOLC1 was shown to be strongly associated with DFS in THCA patients and could be a clinically independent prognostic factor. Further, low NOLC1 expression was strongly related to clinical grade, race, lymph node stage, and gender of THCA patients. In addition, our study analyzed genes with correlations to NOLC1, which will help to explore further the specific molecular mechanisms of NOLC1 low expression in THCA. Functional enrichment analysis showed that the pathways, including ribosome generation, antigen processing and presentation, and cell morphology, were related to NOLC1 expression. NOLC1 may affect the progression and prognosis of THCA patients by altering the tumor's immune microenvironment. Finally, low NOLC1 expression was experimentally confirmed to play a pathogenic role in THCA. We confirmed the association between NOLC1 expression and THCA by bioinformatics analysis and *in vivo* and *in* vitro experiments. This will facilitate the identification of new tumor markers, drug development, and improvement of treatment strategies.

## Acknowledgements

This research was funded by the Youth Science and technology innovation leader of Ningbo (No. 2023QL052), the National Natural Science Foundation of Zhejiang (No. LY24C050001), the National Natural Science Foundation of China (No. 32270821), the Natural Science Foundation of Ningbo (No. 2021J065), the Na-

tural Science Foundation of Zhejiang Province (LTGY24H160004), and the K.C. Wong Magna Fund in Ningbo University.

## Disclosure of conflict of interest

None.

**Address correspondence to:** Meng Ye and Xiaofeng Jin, The First Hospital of Ningbo University, Ningbo 315010, Zhejiang, China. E-mail: yemeng@nbu.edu.cn (MY); jinxiaofeng@nbu.edu.cn (XFJ)

## References

[1] Gonçalves CFL, Hecht F, Cazarin J, Fortunato RS, Vaisman M, Carvalho DP and Ferreira ACF. The flavonoid quercetin reduces cell migration and increases NIS and E-cadherin mRNA in the human thyroid cancer cell line BCPAP. Mol Cell Endocrinol 2021; 529: 111266.

[2] Xing M, Haugen BR and Schlumberger M. Progress in molecular-based management of differentiated thyroid cancer. Lancet 2013; 381: 1058-1069.

[3] Haugen BR and Sherman SI. Evolving approaches to patients with advanced differentiated thyroid cancer. Endocr Rev 2013; 34: 439-455.

[4] Yang Q, Cheng J, Liu Y, Hong Y, Wang JJ and Zhang SL. Cloning and identification of NS5ATP2 gene and its spliced variant transactivated by hepatitis C virus non-structural protein 5A. World J Gastroenterol 2004; 10: 1735-1739.

[5] Zhai F, Wang J, Luo X, Ye M and Jin X. Roles of NOLC1 in cancers and viral infection. J Cancer Res Clin Oncol 2023; 149: 10593-10608.

[6] Sun Z, Zhang Q, Lv J, Sun Y, Feng Z, Zhang M, Zhang F, Xia C, Gao Y, Zhang Z, Zuo YF and Ren SY. High expression of NOLC1 as an independent prognostic factor for survival in patients with colorectal cancer. J Cancer Res Clin Oncol 2023; 149: 15697-15712.

[7] Kim W, Yeo DY, Choi SK, Kim HY, Lee SW, Ashim J, Han JE, Yu W, Jeong H, Park JK and Park S. NOLC1 knockdown suppresses prostate cancer progressions by reducing AKT phosphorylation and β-catenin accumulation. Biochem Biophys Res Commun 2022; 635: 99-107.

[8] Wu CY, Li L, Chen SL, Yang X, Zhang CZ and Cao Y. A Zic2/Runx2/NOLC1 signaling axis mediates tumor growth and metastasis in clear cell renal cell carcinoma. Cell Death Dis 2021; 12: 319.

[9] Zhu CY, Zheng FL, She XS, Zhao D, Gu Y, Duan YT, Chang AK and Liu HS. Identification of NS1 domains of avian H5N1 influenza virus which influence the interaction with the NOLC1 protein. Virus Genes 2015; 50: 238-244.

[10] Hwang YC, Lu TY, Huang DY, Kuo YS, Kao CF, Yeh NH, Wu HC and Lin CT. NOLC1, an enhancer of nasopharyngeal carcinoma progression, is essential for TP53 to regulate MDM2 expression. Am J Pathol 2009; 175: 342-354.

[11] Yuan F, Zhang Y, Ma L, Cheng Q, Li G and Tong T. Enhanced NOLC1 promotes cell senescence and represses hepatocellular carcinoma cell proliferation by disturbing the organization of nucleolus. Aging Cell 2017; 16: 726-737.

[12] Zhen J, Song Z, Su W, Zeng QC, Li J and Sun Q. Integrated analysis of RNA-binding proteins in thyroid cancer. PLoS One 2021; 16: e0247836.

[13] Zhang S, Zhang E, Long J, Hu Z, Peng J, Liu L, Tang F, Li L, Ouyang Y and Zeng Z. Immune infiltration in renal cell carcinoma. Cancer Sci 2019; 110: 1564-1572.

[14] Hu J, Yuan IJ, Mirshahidi S, Simental A, Lee SC and Yuan X. Thyroid carcinoma: phenotypic features, underlying biology and potential relevance for targeting therapy. Int J Mol Sci 2021; 22: 1950.

[15] Tang M, Luo W, Zhou Y, Zhang Z and Jiang Z. Anoikis-related gene CDKN2A predicts prognosis and immune response and mediates proliferation and migration in thyroid carcinoma. Transl Oncol 2024; 40: 101873.

[16] Doolittle WKL, Zhao L and Cheng SY. Blocking CDK7-mediated NOTCH1-cMYC signaling attenuates cancer stem cell activity in anaplastic thyroid cancer. Thyroid 2022; 32: 937-948.

[17] Yuan F, Li G and Tong T. Nucleolar and coiled-body phosphoprotein 1 (NOLC1) regulates the nucleolar retention of TRF2. Cell Death Discov 2017; 3: 17043.

[18] Celli GB and de Lange T. DNA processing is not required for ATM-mediated telomere damage response after TRF2 deletion. Nat Cell Biol 2005; 7: 712-718.

[19] Werner A, Iwasaki S, McGourty CA, Medina-Ruiz S, Teerikorpi N, Fedrigo I, Ingolia NT and Rape M. Cell-fate determination by ubiquitin-dependent regulation of translation. Nature 2015; 525: 523-527.

[20] Yang X and Zhu Q. SPOP in cancer: phenomena, mechanisms and its role in therapeutic implications. Genes (Basel) 2022; 13: 2051.

[21] Zhang H, Jin X and Huang H. Deregulation of SPOP in cancer. Cancer Res 2023; 83: 489-499.

[22] Zuhlke KA, Johnson AM, Tomlins SA, Palanisamy N, Carpten JD, Lange EM, Isaacs WB and Cooney KA. Identification of a novel germline SPOP mutation in a family with hereditary prostate cancer. Prostate 2014; 74: 983-990.

[23] Li G, Ci W, Karmakar S, Chen K, Dhar R, Fan Z, Guo Z, Zhang J, Ke Y, Wang L, Zhuang M, Hu S,

Li X, Zhou L, Li X, Calabrese MF, Watson ER, Prasad SM, Rinker-Schaeffer C, Eggener SE, Stricker T, Tian Y, Schulman BA, Liu J and White KP. SPOP promotes tumorigenesis by acting as a key regulatory hub in kidney cancer. Cancer Cell 2014; 25: 455-468.

[24] Gao X, Wang Q, Li W, Yang B, Song H, Ju W, Liu S and Cheng J. Identification of nucleolar and coiled-body phosphoprotein 1 (NOLC1) minimal promoter regulated by NF-κB and CREB. BMB Rep 2011; 44: 70-75.

[25] Bremnes RM, Al-Shibli K, Donnem T, Sirera R, Al-Saad S, Andersen S, Stenvold H, Camps C and Busund LT. The role of tumor-infiltrating immune cells and chronic inflammation at the tumor site on cancer development, progression, and prognosis: emphasis on non-small cell lung cancer. J Thorac Oncol 2011; 6: 824-833.

[26] Lu Y, Zhao Q, Liao JY, Song E, Xia Q, Pan J, Li Y, Li J, Zhou B, Ye Y, Di C, Yu S, Zeng Y and Su S. Complement signals determine opposite effects of B cells in chemotherapy-induced immunity. Cell 2020; 180: 1081-1097, e1024.

[27] Kryczek I, Banerjee M, Cheng P, Vatan L, Szeliga W, Wei S, Huang E, Finlayson E, Simeone D, Welling TH, Chang A, Coukos G, Liu R and Zou W. Phenotype, distribution, generation, and functional and clinical relevance of Th17 cells in the human tumor environments. Blood 2009; 114: 1141-1149.

[28] Tosolini M, Kirilovsky A, Mlecnik B, Fredriksen T, Mauger S, Bindea G, Berger A, Bruneval P, Fridman WH, Pagès F and Galon J. Clinical impact of different classes of infiltrating T cytotoxic and helper cells (Th1, th2, treg, th17) in patients with colorectal cancer. Cancer Res 2011; 71: 1263-1271.

[29] Wen PY, Stein A, van den Bent M, De Greve J, Wick A, de Vos FYFL, von Bubnoff N, van Linde ME, Lai A, Prager GW, Campone M, Fasolo A, Lopez-Martin JA, Kim TM, Mason WP, Hofheinz RD, Blay JY, Cho DC, Gazzah A, Pouessel D, Yachnin J, Boran A, Burgess P, Ilankumaran P, Gasal E and Subbiah V. Dabrafenib plus trametinib in patients with BRAF(V600E)-mutant low-grade and high-grade glioma (ROAR): a multicentre, open-label, single-arm, phase 2, basket trial. Lancet Oncol 2022; 23: 53-64.

[30] Saronni D, Gaudenzi G, Dicitore A, Carra S, Cantone MC, Borghi MO, Barbieri A, Mignani L, Hofland LJ, Persani L and Vitale G. Preclinical evaluation of novel tyrosine-kinase inhibitors in medullary thyroid cancer. Cancers (Basel) 2022; 14: 4442.

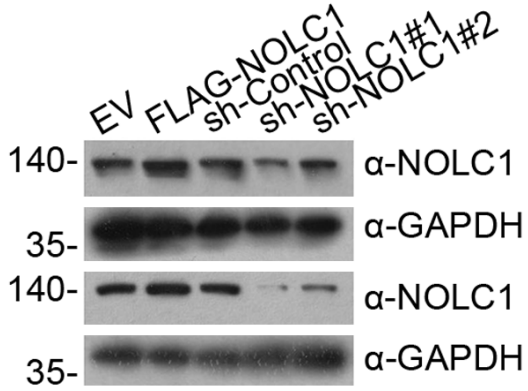


**Supplementary Figure 1.** The sh-RNA knockdown effective of NOLC1 was proved.